Journal of ELECTRONIC MATERIALS, Vol. 40, No. 9, 2011
DOI: 10.1007/s11664-011-1684-z

Electromigration in a Sn-3 wt.%Ag-0.5 wt.%Cu-3 wt.%Bi Solder Stripe Between Two Cu Electrodes Under Current Stressing

SHANG-HUA LEE[1] and CHIH-MING CHEN[1,2,3]

1.—Department of Chemical Engineering, National Chung Hsing University, Taichung 402, Taiwan. 2.—e-mail: chencm@nchu.edu.tw. 3.—e-mail: chencm@dragon.nchu.edu.tw

The electromigration behavior of a Sn-3 wt.%Ag-0.5 wt.%Cu-3 wt.%Bi solder stripe between two Cu electrodes under current stressing at various densities has been investigated for a current stressing time of 72 h and a temperature of 120°C. After current stressing at a density of 1.0×10^4 A/cm^2, the solder matrix exhibited a slight microstructural change as well as formation of a distributed Cu_6Sn_5 phase near the anode-side solder/Cu interface. Upon increasing the current density to 3.9×10^4 A/cm^2 and 5.0×10^4 A/cm^2, a high density of distributed Cu_6Sn_5 phase was formed across the entire solder stripe, resulting in pronounced microstructural change of the solder. Hillocks were also formed near the anode-side interface due to accumulation of a Sn-rich phase, a Bi-rich phase, and a distributed Cu_6Sn_5 phase, while voids were formed in the solder matrix and at the opposite cathode side. The mechanisms of formation of the distributed Cu_6Sn_5 phase and migration of Bi and Sn are discussed.

Key words: Electromigration, solder, Cu, microstructure

INTRODUCTION

SnAgCu-based solder (such as Sn-3 wt.%Ag-0.5 wt.%Cu) has been the most popular Pb-free solder for consumer electronics packaging to date. However, this solder still has some physical and chemical properties that need improvement; for example, its melting point (~217°C) is higher than that of conventional Sn-37 wt.%Pb solder (183°C), making direct application of this solder in the traditional reflow process (used for Sn-37 wt.%Pb solder) more inconvenient and difficult. In addition, the high Sn content of SnAgCu solder enhances growth of Sn-based intermetallic compounds at solder joints, which degrades their mechanical strength.

Addition of a fourth element to SnAgCu solder is a method commonly used to improve the solder's physical or chemical properties. It is reported that a small amount of Bi addition to SnAgCu solder can reduce the melting point of the solder[1,2] and lower the growth rate of Sn-based intermetallic compounds at the solder joint.[3,4] Generally, the amount of Bi added is less than 3 wt.%, because more Bi addition is disadvantageous to the mechanical properties of the solder due to the brittle nature of Bi.

Miniaturization is a global trend in consumer electronics because the need for smaller, lighter, and portable electronics is increasing. However, scale reduction of electronic products increases the current density in solder joints, resulting in enhanced electromigration effects, which can cause reliability problems.[5–10] Electromigration refers to the phenomenon of directional atomic movement induced by current stressing,[11,12] which can induce significant microstructural changes, such as void and hillock formation and phase segregation, and affect growth of intermetallic compounds in solder joints.[13–17]

To the best of our knowledge, electromigration in Bi-added SnAgCu solder has not been reported to date. So, this present study aims to explore electromigration in Sn-3 wt.%Ag-0.5 wt.%Cu solder with 3 wt.% added Bi. A thin stripe-type sample was prepared, and the solder was placed between two Cu electrodes. Due to the thin stripe configuration, the

(Received November 7, 2010; accepted May 23, 2011; published online June 21, 2011)

current density could be increased to the range of 10^4 A/cm^2 to 10^5 A/cm^2, enabling investigation of solder electromigration under high current density.

EXPERIMENTAL PROCEDURES

A Cu/Ta bilayer was deposited on a SiO_2/Si substrate using sputtering. The thickness of Cu and Ta was 4000 Å and 200 Å, respectively. The Cu layer was then grown to 10 μm thick using electroplating. Using photolithography and lift-off techniques, the Cu/Ta bilayer was patterned to a stripe with a square pad at each end. The dimensions of the stripe were 10 mm in length and 300 μm in width. Using photolithography and lift-off techniques for the second time, a trench with a length of 500 μm was patterned in the middle of the stripe. The trench was designed to be filled with solder. To improve wettability, the trench was designed to have a depth of 9.6 μm, so that a thin Cu layer with a thickness of 4000 Å remained at the bottom of the trench. A tiny solder piece (Sn-3 wt.%Ag-0.5 wt.%Cu-3 wt.%Bi) coated with flux was placed in the trench. The sample was reflowed at 250°C for 3 s to 5 s and then cooled to room temperature. After reflow, the solder piece was transformed into a bump in the trench of the Cu stripe, being joined to the Cu stripe at its two ends. By careful polishing using ultrafine sandpapers and 0.3-μm Al_2O_3 suspension, the solder bump was polished down until the solder thickness was the same as the Cu stripe. The sample configuration and the experimental setup were shown schematically elsewhere.[18]

To perform the electromigration experiment, a direct-current power supply was connected to the Cu stripe at its two end pads to provide current density ranging from 1.0×10^4 A/cm^2 to 5.0×10^4 A/cm^2. A thermocouple was attached to the Cu stripe to monitor the temperature during the electromigration test. Owing to Joule heating, the sample was heated as the current passed though it. The thermocouple revealed that the temperature rose rapidly and stayed around 60 ± 3°C after 30 min of current stressing. By turning on the hot plate and controlling the output power carefully, the samples were heated again to the desired temperature of 120°C. After electromigration, the microstructural change of the solder surface was examined by scanning electron microscopy (SEM). Composition analysis was carried out by energy-dispersive x-ray spectrometry (EDX). To identify the electromigration effect, a reference experiment was conducted, where the sample was only annealed in a 120°C oven for the same time (without current stressing).

RESULTS AND DISCUSSION

Figure 1a shows a top-view SEM micrograph of the as-prepared sample. The solder surface was flat except for the formation of some small voids in the solder matrix. It was found that the solder joined well with the Cu electrodes at its two ends. Careful observation revealed that a thin ($\sim$2 μm) intermetallic compound was formed at the solder/Cu interface on both sides, being identified as Cu_6Sn_5 according to compositional analysis by EDX. After current stressing (1.0×10^4 A/cm^2) at 120°C for 72 h, the solder exhibited a slight microstructural change as seen in Fig. 1b, c, where the electrons flowed from the right-hand side (cathode) to the left-hand side (anode). Figure 1b was taken in secondary-electron image (LEI) mode to reveal

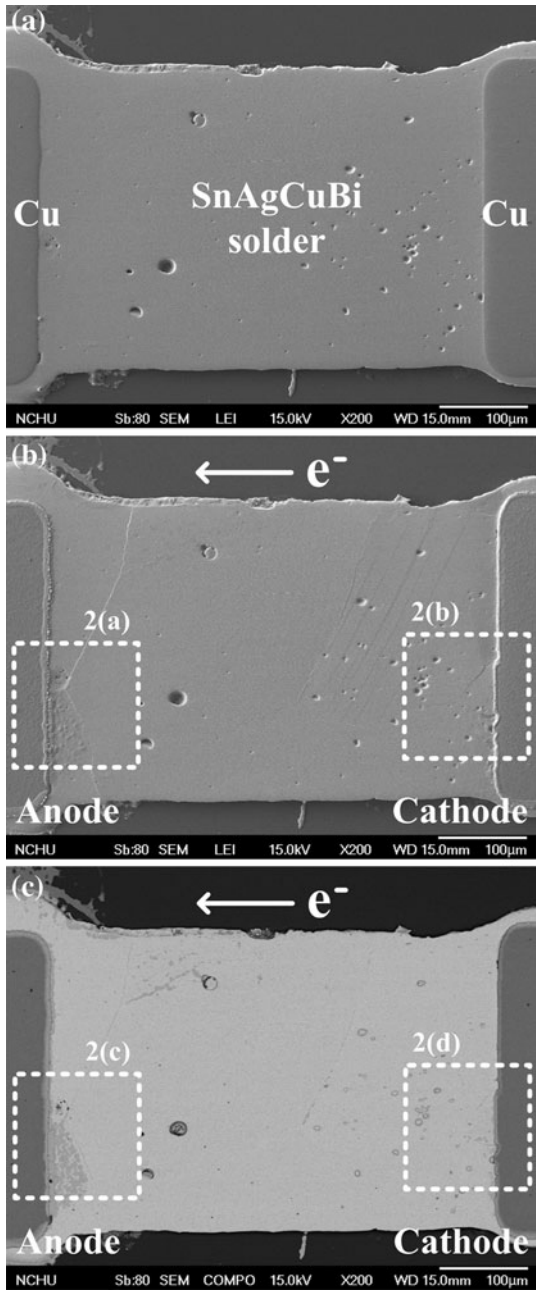

Fig. 1. Top-view SEM micrographs of (a) the as-prepared sample, (b) the sample after current stressing (1.0×10^4 A/cm^2) at 120°C for 72 h in LEI mode, and (c) the sample after current stressing (1.0×10^4 A/cm^2) at 120°C for 72 h in BEI mode.

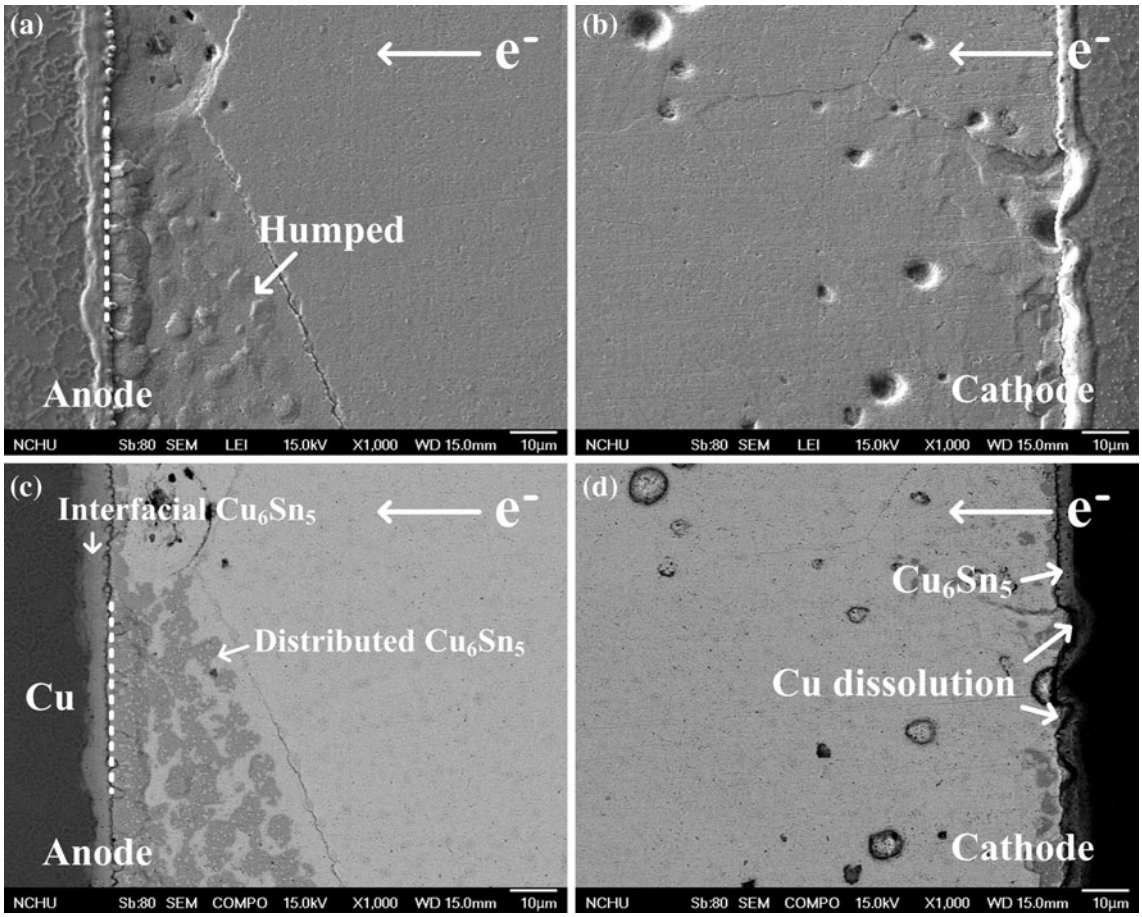

Fig. 2. High-magnification SEM micrographs of the anode-side and cathode-side interfaces of the sample shown in Fig. 1b, c.

morphological changes of the solder surface, while Fig. 1c was taken in backscattered electron image mode (BEI) to clearly show the distinction between the different phases.

As seen in Fig. 1b, c, the microstructures of the solder surface at the anode and cathode sides were different. High-magnification micrographs of these two sides are shown in Fig. 2a–d. The Cu_6Sn_5 phase formed at the solder/Cu interfaces grew thicker, and its humped morphology (Fig. 2a, b) indicates that its formation resulted in volume expansion at the solder/Cu interface. Many humped sites were also formed in the solder near the anode-side interface, as seen in Fig. 2a. In the corresponding BEI-mode micrograph (Fig. 2c), these humped sites exhibited similar color and contrast to the interfacial Cu_6Sn_5 phase. According to EDX compositional analysis, they were also identified as Cu_6Sn_5. To differentiate them, a dotted line was drawn between them. To the left of the dotted line, the Cu_6Sn_5 phase was formed at the solder/Cu interface, being called the interfacial Cu_6Sn_5 phase. To the right of the dotted line, the Cu_6Sn_5 phase is located in the solder matrix and is called the distributed Cu_6Sn_5 phase due to its distribution and discontinuity. The interfacial Cu_6Sn_5 phase has a continuous layered structure, while the distributed Cu_6Sn_5 phase is of irregular shape.

Figure 3 shows a series of SEM micrographs of the sample after only annealing at 120°C for 72 h (without current stressing). The LEI-mode micrograph (Fig. 3a) reveals that the solder surface is still flat, and the BEI-mode micrograph (Fig. 3b–d) indicates that no noticeable distributed Cu_6Sn_5 phase is formed within the solder matrix. Compared with the results shown in Figs. 1 and 2, electromigration affects the microstructure evolution of the Bi-added SnAgCu solder under the current stressing condition used in this work.

Another obvious distinction between the interfacial and distributed Cu_6Sn_5 phase in Fig. 2c is that many small gray-white particles are embedded in the distributed Cu_6Sn_5 phase. The small gray-white particles were identified as Ag_3Sn. They are suggested to precipitate during solder solidification because they were observed in the as-solidified solder. Precipitation of small Ag_3Sn particles in SnAgCu-based solder was also observed elsewhere.[19] In contrast, no Ag_3Sn precipitates were found in the interfacial Cu_6Sn_5 phase. It is suggested that the formation of the interfacial Cu_6Sn_5 phase is governed by diffusion of Sn from the solder

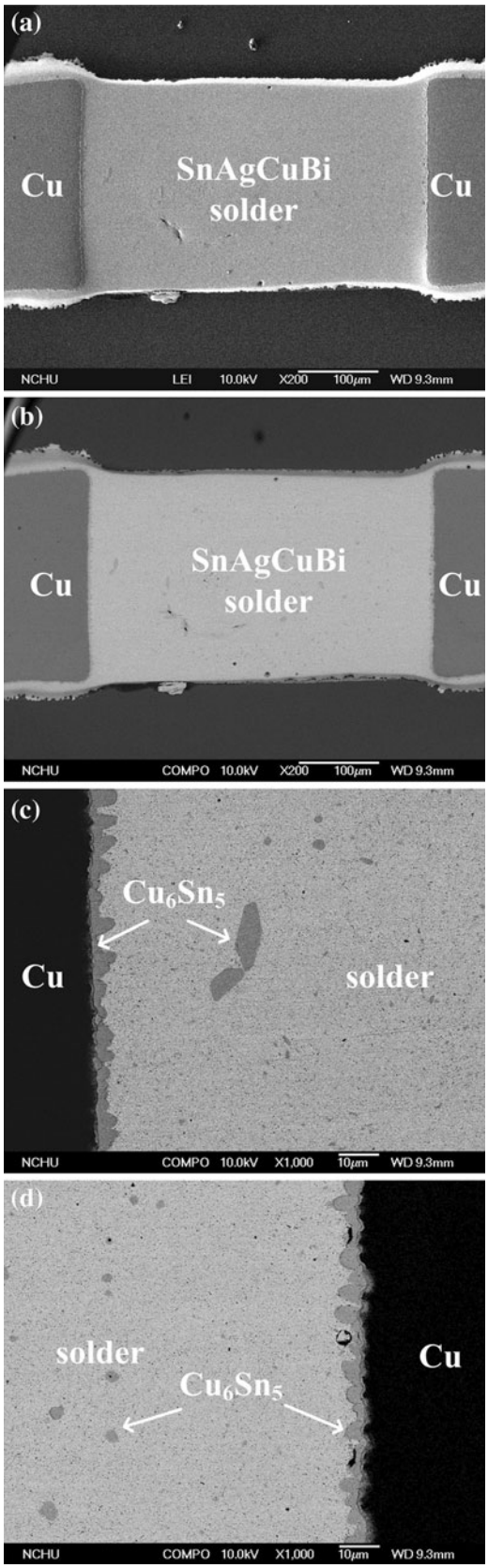

Fig. 3. A series of SEM micrographs of the sample after only annealing at 120°C for 72 h (without current stressing): (a) LEI- and (b) BEI-mode images of the entire sample, and (c, d) BEI-mode images of the solder/Cu interfaces at the two ends.

side to the Cu side to transform the Cu electrode into Cu_6Sn_5 via the Sn/Cu interfacial reaction. Because the Cu electrode is originally free of Ag_3Sn precipitates, the Cu_6Sn_5 phase formed from the Cu electrode is also free of Ag_3Sn precipitates. The driving forces for Sn diffusion include the intrinsic concentration gradient and the extrinsic electromigration force, because the direction of Sn diffusion is the same as that of electron flow. In contrast, the distributed Cu_6Sn_5 phase formed in the solder matrix is governed by the diffusion of Cu from the Cu electrode to the solder matrix. When the Cu atoms diffuse into the solder matrix, they react with the Sn atoms and form Cu_6Sn_5. Because the solder is composed of a Sn-rich matrix and many small Ag_3Sn precipitates, the formation of the distributed Cu_6Sn_5 phase in the Sn matrix accompanies the embedment of the Ag_3Sn precipitates.

In our samples, the Cu atoms have two sources: the nearby anode-side Cu electrode and the Cu electrode at the far-end cathode side. If the Cu atoms contributing to the formation of the distributed Cu_6Sn_5 phase come from the nearby anode-side Cu electrode, the distributed Cu_6Sn_5 phase could also form near the cathode side by virtue of the diffusion of Cu from the cathode-side Cu electrode. However, the distributed Cu_6Sn_5 phase was hardly seen near the cathode side, as seen in Fig. 2d. This indicates that the concentration gradient is not the primary driving force for Cu diffusion. As mentioned above, electromigration is also a driving force for atomic diffusion. In electromigration, the Cu atoms migrate from the cathode side to the anode side. From Fig. 2d, some localized Cu dissolution sites were found at the interface. Therefore, it is suggested that electromigration induces Cu dissolution from the cathode-side Cu electrode and then drives the dissolved Cu atoms to migrate toward the anode side. When the dissolved Cu atoms arrive at the anode side, they react with the Sn atoms and form many regions of distributed Cu_6Sn_5 phase.

When the current density was increased to 3.9×10^4 A/cm^2, a large amount of distributed Cu_6Sn_5 phase was formed in the solder matrix, as seen in Fig. 4a, b. This indicates that the enhanced electromigration force induced more Cu dissolution from the cathode-side Cu electrode into the solder matrix to form the distributed Cu_6Sn_5 phase. At the anode side, the distributed Cu_6Sn_5 phase even accumulated to form a continuous layer along the interface as seen in Fig. 4a. Hillocks and voids were found at the anode and cathode sides, respectively. In addition, bright Bi particles were found near the anode side, revealing that Bi atoms migrated toward the anode side under electromigration. The phenomenon of directional migration of Bi under electromigration was also observed in other Bi-bearing solder alloys such as Sn-58 wt.%Bi[20,21] and Sn-8 wt.%Zn-3 wt.%Bi.[22] The Bi particles segregate behind (to the right of) the accumulated layer of the distributed Cu_6Sn_5 phase, meaning that migration of Cu is

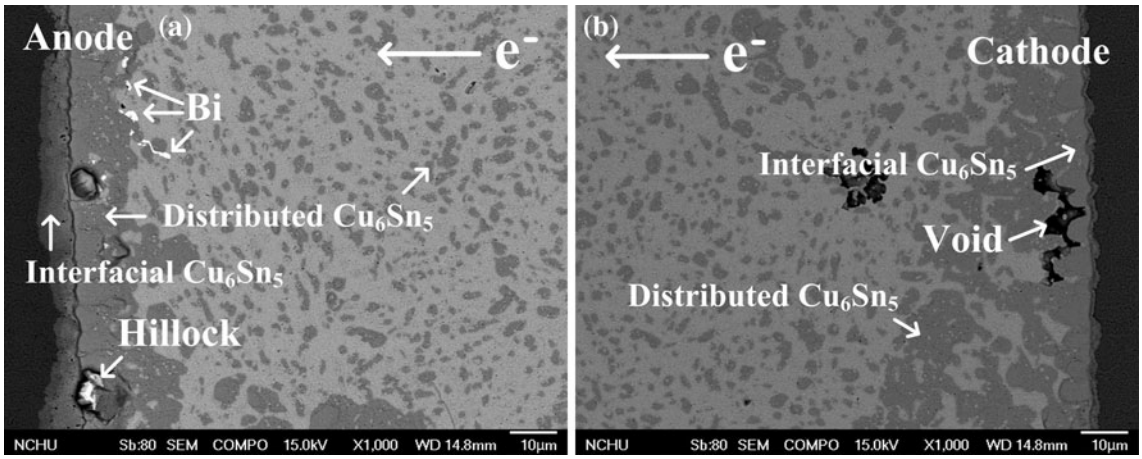

Fig. 4. Top-view SEM micrographs of the sample after current stressing (3.9×10^4 A/cm^2) at 120°C for 72 h: (a) anode-side interface, and (b) cathode-side interface.

faster than that of Bi in the solder matrix. The faster migration of Cu in the solder (Sn) matrix is attributed to the interstitial diffusion mechanism due to the smaller size of Cu in comparison with Sn.

Figure 5 shows top-view SEM micrographs of the sample after current stressing at the highest density of 5.0×10^4 A/cm^2 at 120°C for 72 h. Many hillocks were formed at the anode-side interface, while the solder sank at the cathode side, as seen in Fig. 5a. The solder matrix also humped slightly at many sites. In the BEI-mode SEM micrograph shown in Fig. 5b, the slightly humped morphology is attributed to the formation of a high-density of the distributed Cu_6Sn_5 phase in the solder matrix. In contrast, solder stressed at a lower current density of 1.0×10^4 A/cm^2 (Fig. 1b, c) did not exhibit noticeable morphological changes across the entire solder matrix, except for the slight hump near the anode-side interface. The humped morphology in Fig. 1b was also caused by the formation of the distributed Cu_6Sn_5 phase. In comparison with the solder stressed at 3.9×10^4 A/cm^2, the current density of 5.0×10^4 A/cm^2 induces more Cu dissolution from the cathode-side Cu electrode into the solder matrix, and accordingly results in the formation of a higher-density of the distributed Cu_6Sn_5 phase. In Fig. 5b, no localized Cu dissolution sites like those seen in Fig. 2d were found. It is suggested that the Cu dissolution occurred evenly along the entire interface for the higher current density, so that no localized Cu dissolution sites were formed.

Figure 5c and d show high-magnification micrographs of the anode-side and cathode-side interfaces, respectively. It is found that the hillock formed near the anode-side interface is composed of Sn, distributed Cu_6Sn_5 phase, and Bi. It is of interest to determine the primary cause of hillock formation. By polishing the sample until the hillocks were removed, the solder was found to exhibit an interesting microstructure near the anode-side interface, as seen in Fig. 6. The distributed Cu_6Sn_5 phase disappears, but a Sn-rich region (nearly free of distributed Cu_6Sn_5 phase) is found instead at the right-hand side of the interface. This indicates that Sn atoms in the solder matrix also migrate toward the anode side under electromigration. Electromigration-induced Sn migration appears to overwhelm Cu migration in the interior of the solder, so the Sn atoms accumulate toward the anode-side interface prior to the arrival of the Cu atoms. As a result, the distributed Cu_6Sn_5 phase was hardly formed in the vicinity of the anode-side interface. More voids were found in the solder matrix, which also provides evidence for Sn migration. The Sn migration results in atomic accumulation near the anode-side interface. Therefore, compressive stress is built up, which induces the hillock formation.[16,23,24]

Figure 7 shows a SEM micrograph of the solder matrix after current stressing. Two kinds of Cu_6Sn_5 phase were found. One has a hexagonal appearance and the other is irregularly shaped. Detailed observation reveals that the hexagonal-shaped Cu_6Sn_5 phase is pure Cu_6Sn_5 without small embedded Ag_3Sn precipitates, whereas many small Ag_3Sn precipitates are embedded in the irregular-shaped Cu_6Sn_5 phase. As mentioned above, the irregular-shaped Cu_6Sn_5 phase with small embedded Ag_3Sn precipitates was formed by the dissolution of the Cu electrode at the cathode side under electromigration. It is suggested that the hexagonal-shaped Cu_6Sn_5 phase precipitated during solder solidification, because it was observed before the electromigration experiment. The observation of the hexagonal-shaped Cu_6Sn_5 phase in the as-solidified solder is consistent with another study.[25]

To understand the effect of Bi addition on the electromigration of solder, we conducted an additional EM experiment using SAC305 solder (without Bi addition). A SEM micrograph of the solder after current stressing (5.0×10^4 A/cm^2, 120°C, 72 h) is shown in Fig. 8. Compared with the Bi-added SAC305 solder shown in Fig. 5b, the density of

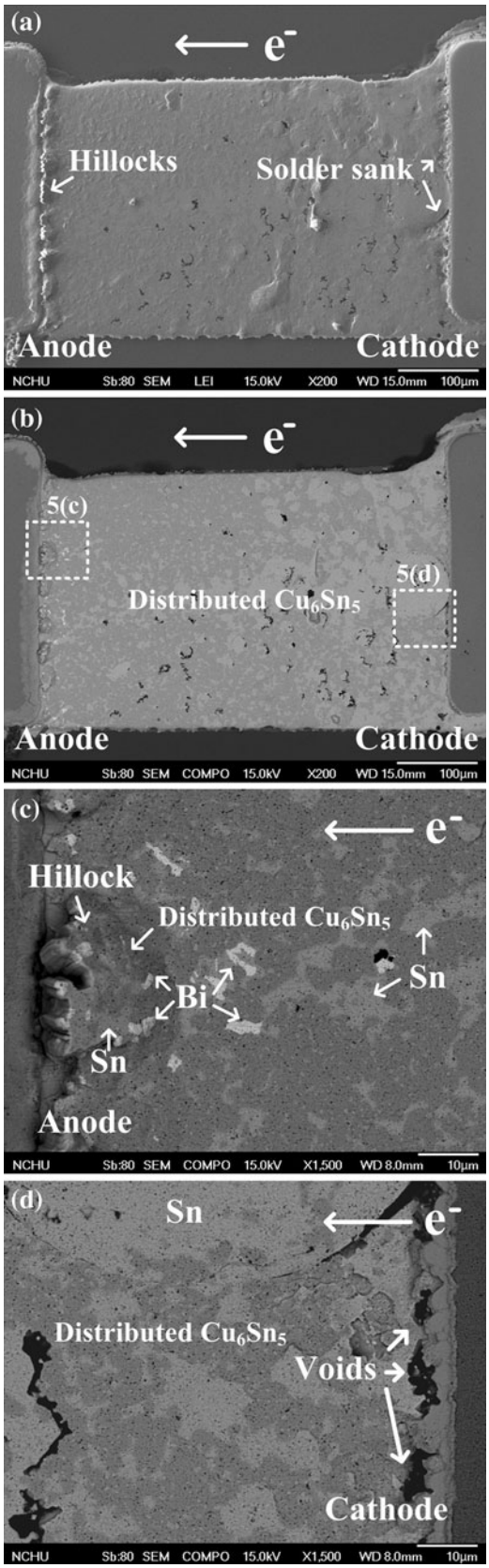

Fig. 5. Top-view SEM micrographs of the sample after current stressing (5.0×10^4 A/cm^2) at 120°C for 72 h in (a) LEI mode and (b) BEI mode, and high-magnification micrographs of the (c) anode-side and (d) cathode-side interfaces.

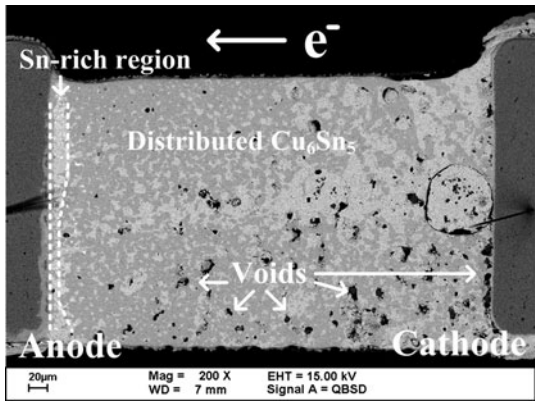

Fig. 6. Top-view SEM micrograph of the sample shown in Fig. 5b with the hillocks at the anode-side interface completely removed.

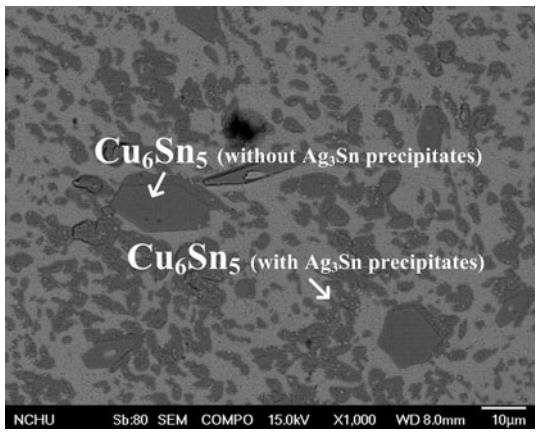

Fig. 7. SEM micrograph of the solder matrix after current stressing.

the distributed Cu_6Sn_5 phase formed within the SAC305 solder is much lower. In other words, the addition of Bi to the SAC305 solder enhances the electromigration effect, resulting in the formation of a large amount of distributed Cu_6Sn_5 phase within the solder (Fig. 5b). Zhao et al. found that the addition of Bi (3 wt.%) to SAC305 solder significantly reduced the size of the Sn-rich phase.[1] In this study, we also observed size reduction of the Sn-rich phase when Bi was added to SAC305 solder, as seen in Fig. 9. In addition, the density of the eutectic structure (dark regions surrounding the Sn-rich phase in Fig. 9) was increased by the addition of Bi. It is suggested that the density of grain/interphase boundaries in the Bi-added solder is increased due to grain size reduction and eutectic increment, thereby facilitating electromigration-induced Cu diffusion in the solder. Therefore, a large quantity of the distributed Cu_6Sn_5 phase was formed within the solder.

CONCLUSIONS

Electromigration has significant effects on the microstructural evolution of Sn-3 wt.%Ag-0.5 wt.%Cu-3 wt.%Bi solder. Under current stressing

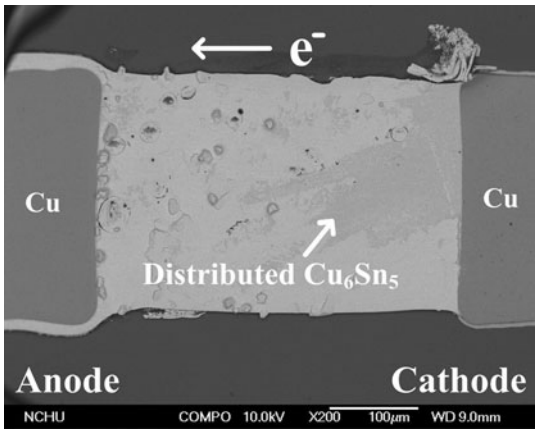

Fig. 8. Top-view SEM micrograph of the sample after current stressing (5.0×10^4 A/cm^2) at 120°C for 72 h. The solder is SAC305 without addition of Bi.

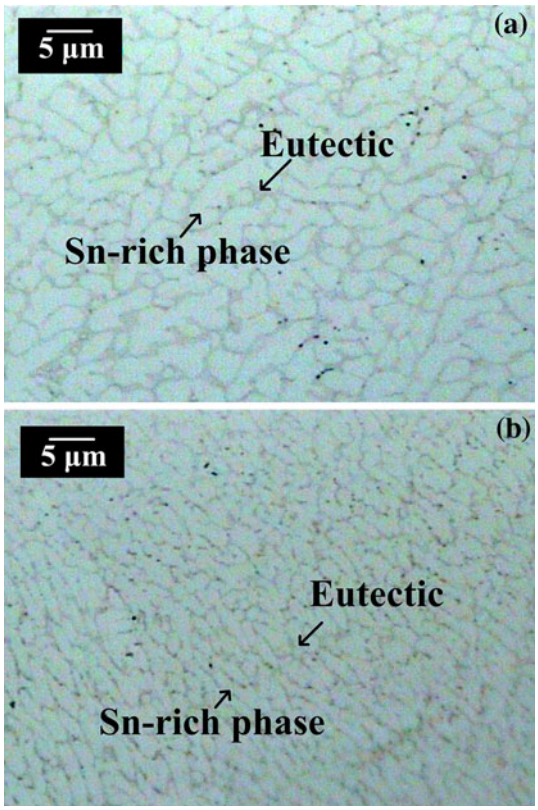

Fig. 9. Optical micrographs of (a) SAC305 and (b) Bi-added SAC305 solders.

at a density of 1.0×10^4 A/cm^2, the electromigration force induces local dissolution of the cathode-side Cu electrode. The dissolved Cu atoms migrate along with the electron flow toward the anode side and form a small amount of a distributed Cu_6Sn_5 phase near the anode-side solder/Cu interface. Additionally, an interfacial Cu_6Sn_5 phase is formed at the solder/Cu interface. Many small Ag_3Sn precipitates are embedded in the distributed Cu_6Sn_5 phase, but the interfacial Cu_6Sn_5 phase is free of embedded Ag_3Sn precipitates. When the current density is increased to 3.9×10^4 A/cm^2 or 5.0×10^4 A/cm^2, more Cu atoms dissolve into the solder matrix and form a high density of the distributed Cu_6Sn_5 phase across the entire solder matrix. Electromigration also induces directional migration of Sn and Bi toward the anode-side interface, which results in hillock growth, while voids are formed in the solder matrix and at the cathode side.

ACKNOWLEDGEMENTS

The authors gratefully acknowledge the financial support of the National Science Council of Taiwan under Grants NSC 96-2221-E-005-064-MY3 and NSC 99-2628-E-005-006. This work is supported in part by the Ministry of Education, Taiwan, R.O.C. under the ATU plan.

REFERENCES

1. J. Zhao, L. Qi, X.M. Wang, and L. Wang, *J. Alloys Compd.* 375, 196 (2004).
2. Y. Kariya and M. Otsuka, *J. Electron. Mater.* 27, 866 (1998).
3. M.J. Rizvi, Y.C. Chan, C. Bailey, H. Lub, and M.N. Islam, *J. Alloys Compd.* 407, 208 (2006).
4. L. Qi, J. Zhao, X.M. Wang, and L. Wang, *IEEE International Conference on the Business of Electronic Product Reliability and Liability* (2004), p. 42.
5. W.J. Choi, E.C.C. Yeh, and K.N. Tu, *J. Appl. Phys.* 94, 5665 (2003).
6. S.W. Chen, S.K. Lin, and J.M. Jao, *Mater. Trans.* 45, 661 (2004).
7. T.Y. Lee and K.N. Tu, *J. Appl. Phys.* 89, 3189 (2001).
8. J.W. Nah, K.W. Paik, J.O. Suh, and K.N. Tu, *J. Appl. Phys.* 94, 7560 (2003).
9. S.S. Ha, J.W. Kim, J.W. Yoon, S.O. Ha, and S.B. Jung, *J. Electron. Mater.* 38, 70 (2008).
10. L. Xu, J.K. Han, J.J. Liang, K.N. Tu, and Y.S. Lai, *Appl. Phys. Lett.* 92, 262104 (2008).
11. H.B. Huntington and A.R. Grone, *J. Phys. Chem. Solids* 20, 76 (1961).
12. J.R. Black, *IEEE Trans. Electron Dev.* ED-16, 338 (1969).
13. C.M. Chen and S.W. Chen, *Acta Mater.* 50, 2461 (2002).
14. H. Gan, W.J. Choi, G. Xu, and K.N. Tu, *JOM* 54, 34 (2002).
15. C.M. Chen, L.T. Chen, and Y.S. Lin, *J. Electron. Mater.* 36, 168 (2007).
16. H. He, G. Xu, and F. Guo, *J. Mater. Sci.* 45, 334 (2010).
17. C. Chen, H.M. Tong, and K.N. Tu, *Annu. Rev. Mater. Res.* 40, 531 (2010).
18. Y.M. Hung and C.M. Chen, *J. Electron. Mater.* 37, 887 (2008).
19. A. Zribi, A. Clark, L. Zavalij, P. Borgesen, and E.J. Cotts, *J. Electron. Mater.* 30, 1157 (2001).
20. L.T. Chen and C.M. Chen, *J. Electron. Mater.* 21, 962 (2006).
21. Q.L. Yang and J.K. Shang, *J. Electron. Mater.* 34, 1363 (2005).
22. C.M. Chen, Y.M. Hung, and C.H. Lin, *J. Alloys Compd.* 475, 238 (2009).
23. F.Y. Ouyang, K. Chen, K.N. Tu, and Y.S. Lai, *Appl. Phys. Lett.* 91, 231919 (2007).
24. K. Chen, N. Tamura, M. Kunz, K.N. Tu, and Y.S. Lai, *J. Appl. Phys.* 106, 023502 (2009).
25. B. Li, Y. Shi, Y. Lei, F. Guo, Z. Xia, and B. Zong, *J. Electron. Mater.* 34, 217 (2005).